

MIT Open Access Articles

*Controlling Edge Morphology in Graphene Layers
Using Electron Irradiation: From Sharp Atomic
Edges to Coalesced Layers Forming Loops*

The MIT Faculty has made this article openly available. **Please share**
how this access benefits you. Your story matters.

Citation: Cruz-Silva, E. et al. "Controlling Edge Morphology in Graphene Layers Using Electron Irradiation: From Sharp Atomic Edges to Coalesced Layers Forming Loops." *Physical Review Letters* 105.4 (2010) : 045501. © 2010 The American Physical Society

As Published: <http://dx.doi.org/10.1103/PhysRevLett.105.045501>

Publisher: American Physical Society

Persistent URL: <http://hdl.handle.net/1721.1/60660>

Version: Final published version: final published article, as it appeared in a journal, conference proceedings, or other formally published context

Terms of Use: Article is made available in accordance with the publisher's policy and may be subject to US copyright law. Please refer to the publisher's site for terms of use.



Controlling Edge Morphology in Graphene Layers Using Electron Irradiation: From Sharp Atomic Edges to Coalesced Layers Forming Loops

E. Cruz-Silva,¹ A. R. Botello-Méndez,² Z. M. Barnett,¹ X. Jia,³ M. S. Dresselhaus,³ H. Terrones,² M. Terrones,⁴
B. G. Sumpter,¹ and V. Meunier¹

¹*Oak Ridge National Laboratory, One Bethel Valley Road, Oak Ridge, Tennessee 37831-6367, USA*

²*Université Catholique de Louvain, Place Croix du Sud 1, B-1348 Louvain-la-Neuve, Belgium*

³*Massachusetts Institute of Technology, Cambridge, Massachusetts 02139-4307, USA*

⁴*Carlos III University of Madrid, Avenida Universidad 30, 28911 Leganés, Madrid, Spain*

(Received 21 April 2010; published 22 July 2010)

Recent experimental reports indicate that Joule heating can atomically sharpen the edges of chemical vapor deposition grown graphitic nanoribbons. The absence or presence of loops between adjacent layers in the annealed materials is the topic of a growing debate that this Letter aims to put to rest. We offer a rationale explaining why loops do form if Joule heating is used alone, and why adjacent nanoribbon layers do not coalesce when Joule heating is applied after high-energy electrons first irradiate the sample. Our work, based on large-scale quantum molecular dynamics and electronic-transport calculations, shows that vacancies on adjacent graphene sheets, created by electron irradiation, inhibit the formation of edge loops.

DOI: 10.1103/PhysRevLett.105.045501

PACS numbers: 81.05.ue, 73.63.-b, 83.10.Rs

Graphene can be synthesized by a variety of methods, and subsequently modified by lithographic techniques in order to fabricate electronic devices at the nanoscale [1]. However, variations in thickness (stacked sheets) and edge shape or the presence of defects could significantly modify the electronic properties of graphene. It is therefore imperative to control both the number of stacked layers and edge geometry, in order to optimize the electronic properties and in turn facilitate the design of nanodevices.

Various techniques have been used to engineer and control the atomic structure of carbon nanostructures, such as electron and ion beam irradiation [2], as well as Joule heating [3]. It has been shown that electron irradiation can be effective in removing graphene monolayers from a multilayer material [4]. Subnanometer-scale defects, such as pentagons and heptagons are crucial for creating functional 1D, 2D, and 3D nanomaterials and micromaterials via cross-linking carbon nanotubes [5] and multilayer graphene [6], and by graphene edge reconstruction [7,8]. Important structural changes can also be induced by the controlled knock on of individual carbon atoms, as illustrated recently with aberration-corrected scanning transmission electron microscopy experiments [9]. A number of studies have shown that the *combined* effect of electron irradiation and high temperature could lead to structural modifications and functionalization of sp^2 hybridized carbon nanostructures. For instance, electron irradiation in the TEM at high temperature yields coalesced carbon nanotubes of large diameters [10], molecular junctions [11], and corrugated tubular structures from carbon nanopeapods [12]. In striking contrast to these experiments, where the irradiation is applied locally and the temperature is controlled by heating the entire sample holder, sharp nanoribbon edges are formed when heat is provided by a controlled, directional high electrical current

density after sample exposure to electron irradiation [13]. While the need for local heating has been rationalized using electronic-transport theory [13,14], the role of electron irradiation has been largely ignored in existing models. We also note that experimental studies have reported that loops only form along zigzag edges and not along armchair edges, as observed in highly oriented pyrolytic graphite samples [15].

Treatment by Joule heating alone, i.e., without prior irradiation, enables the reconstruction of individual edges in graphene by creating bilayer and even trilayer looped edges [16], a situation that is also encountered with high temperature thermal treatments [15], in contrast with the results discussed in Ref. [13]. These results may seem contradictory since no explanation has been provided so far to account for loop versus nonloop formation along the edges of graphene structures. It is important to recognize that there are critical differences in the two studies of [13,16], even though the samples were synthesized with identical procedures. Notably, the samples from Ref. [13] were first irradiated for 20 min using an electron beam with a density of 100 A/cm² and accelerated at 200 keV.

In this Letter, we report on an extensive quantum molecular dynamics study of the effect of electron irradiation on graphene, and explain why loops do not form at the edges when fast electrons first irradiate the samples before Joule heating is applied. We use density functional theory (DFT) to demonstrate the previously unclear role of electron irradiation in determining the structural details of graphene bilayer dynamics and how it prevents the formation of layer-to-layer looped edges.

Quantum molecular dynamics (MD) calculations were performed using the Vienna *ab initio* simulation package (VASP) version 4.6.6 [17]. We solved the Kohn-Sham equations using the projected augmented wave method [18] and

the Ceperley-Alder implementation of the local density approximation (LDA) [19] for the exchange and correlation functional. An energy cutoff of 300 eV was used for the plane-wave basis set. The Brillouin zone was sampled with a single k point (Γ), which is well justified given the size of the unit cell. In all the results shown herein, the bilayer graphite was thermalized to 1000 K for 1 ps using a time step of 1 fs for the integration of the equations of motion, while a Nosé thermostat controlled the temperature [20].

The phenomenological interpretation of the role of Joule heating for the experiment reported in Ref. [13] is based on electronic transport and we also complement the present MD calculations with quantum electronic-transport (QET) calculations performed on the final structures obtained after the MD runs. The bilayer nanoribbon structures were considered as four-terminal systems, an approach that allows the separation of in-plane and out-of-plane contributions to the current flow. QET results shown here were performed using the electronic properties obtained with the self-consistent density functional tight binding package DFTB+ [21]. The carbon-carbon interactions were those provided in the Slater-Koster parameter set MATSCI-0-2 [22]. The multiterminal transport properties were calculated using the Landauer-Büttiker formalism [23].

The initial atomic model consists of a 6 unit-cell segment of a 24 Å wide graphene nanoribbon bilayer with zigzag edges and a total of 288 atoms. We performed a series of simulations, corresponding to three different types of irradiation-induced atomic defects: (a) knock-on vacancies, (b) interstitial atoms, and (c) Frenkel pairs (FPs). FPs are made up of a combination of a vacancy and a neighboring interstitial atom [24]. FPs are metastable crystallographic point defects, which are known to be formed on irradiated graphite in nuclear reactors and are in part responsible for the accumulation of the Wigner energy, which is released by transitions to lower-energy configurations, such as Stone-Thrower-Wales defects (i.e., bond rotation) [25], or by interstitial-vacancy annihilation [24].

For experimentally relevant energies and time scales, the nanoribbon open edges are unlikely to be passivated with, e.g., hydrogen. For this reason, we need to be particularly careful about the ring geometry at the open edges (dangling bonds). We determined that for individual layers with zigzag edges that are not saturated by hydrogen, it is energetically more favorable for the hexagons at the edge to reconstruct into 5-7 edges, in agreement with results reported in Ref. [26] for 5-7 edges called “*reczag*” edges [Fig. 1(d)]. Note that when the zigzag edges are saturated with hydrogen, hexagonal edges are preferred and loop formation is precluded by the weak layer-to-layer edge interaction.

The starting system consists of a $\sim 9.7\%$ atomic defect density (i.e., 28 defects for 288 atoms) randomly distributed in the initial graphene nanoribbon bilayer structure. We used a constant set of random vacancies and interstitial

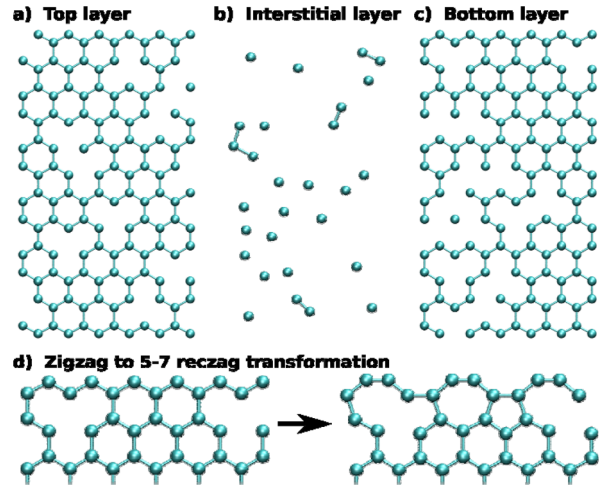


FIG. 1 (color online). Standard set of defects used to model irradiation effects on graphene nanoribbons. Panels (a) and (c) represent the standard vacancies used, and (b) shows the interstitial atoms. Panel (d) shows the edge reconstruction that results in the 5-7 reczag edge.

atom positions shown in Figs. 1(a)–1(c). Both AA (eclipsed) and AB (graphitic) stacking configurations were considered for the zigzag case, while for the reczag case, AA (fully eclipsed), AB (graphitic), and AA′ (eclipsed in the central region, with pentagons overlapping heptagons at the edges) were studied. In total, we investigated 20 different systems (Table I).

In the first series of simulations, we investigated pristine basal planes (no vacancy or FPs). Regardless of the type of stacking, the edges readily close and start looping along the zigzag edges within 200 fs, to form a complete loop before 400 fs. In contrast to hexagonal zigzag edges, reczag edge geometries have a significantly slower kinetics for loop formation. This is because, among the different structures present in the loops, some have high formation energy and are unstable. For instance, for AA stacking, two closing mechanisms are observed: one where the edge is formed by a series of octagons and squares and another where a series of decagons are responsible for the closure. In AB stacking we again observe the decagon closure, and also observe a closure similar to a chain of Stone-Thrower-Wales defects coupled with carbon atoms in bridge positions. A similar observation was made for AA′ stacking.

The second series of calculations involves the introduction of atomic vacancies in the basal planes. Figures 2(a) and 2(b) show the final structure for the zigzag AA and the 5-7 reczag AB structures. We observe an increased layer-layer interaction. While edge loops form swiftly for zigzag edged ribbons [Fig. 2(a)], the effect is greatly reduced for 5-7 reczag ribbons [Fig. 2(b)]. We also observe that, while both layers suffer from distortions during the simulation, they keep a similar shape. The observation of the alignment of a 5-8-5 defect in the reczag AB stacking case [Fig. 2(b)] lends further support to this conclusion. Similar results were observed for other geometries (Table I).

TABLE I. Summary of the different models analyzed with post-MD major features.

Edge shape	Stacking	Pristine	Vacancies	Interstitials	Frenkel pairs
Zigzag	AA	Forms loops after 200 fs.	Few interlayer links, loops after 600 fs.	Monoatomic chains. Loops after 600 fs.	Several diatomic interlayer links. No loops.
	AB				
5-7 reczag	AA	Defective loops formed after 400 fs.	Few interlayer links. No loops.	Monoatomic chains. Interlayer links at 5-7 rings. No loops.	Anchored diatomic links at vacancies. No loops.
	AB				
	AA'				

In the third set of molecular dynamics runs, we initially introduced interstitials in between the otherwise pristine graphene layers [Figs. 2(c) and 2(d)]. The most striking observation is the appearance of atomic chains both between the graphene layers as well as at the edges [Fig. 2(c)]. Some of the interstitial atoms also adsorb as add-atom defects on the graphene layer, thereby acting as anchors for a subsequent chain formation that form bridges between the layers. In the reczag edges, interstitial atoms are found to bind easily to the atoms in heptagons and pentagons [Fig. 2(d)], creating strong bonds that prevent the formation of edge loops.

Finally, we examined the case of the presence of Frenkel pairs in the graphene ribbon. FPs are found to induce a very strong interaction between graphene layers [Fig. 3(a)]. While vacancies confer high reactivity to

the surface, they also enhance anchoring for the interstitial atoms. It follows that monoatomic and diatomic interlayer links develop easily [Fig. 3(b)]. These links are remarkably stable and remain unaltered once fully formed [Figs. 3(c) and 3(d)]. In addition, the presence of these interlayer links eliminates the possibility of loop formation [Figs. 3(b)–3(d)]. The creation of cross-links in these ribbons is consistent with previous findings about the role of FPs in various carbon materials [5,6,24]. It is clear that the major effect of FPs in graphitic materials is cross-linking, which is responsible for keeping graphene layers apart and for hindering the formation of bilayer loop edges.

Previous electronic-transport-based explanations described how Joule heating can sharpen bare edges by inducing high electron transport specifically along the edges of the nanoribbons [13,14]. We now examine how electron transport is affected by the presence of the irradiation-induced defects. In Fig. 4, we show the con-

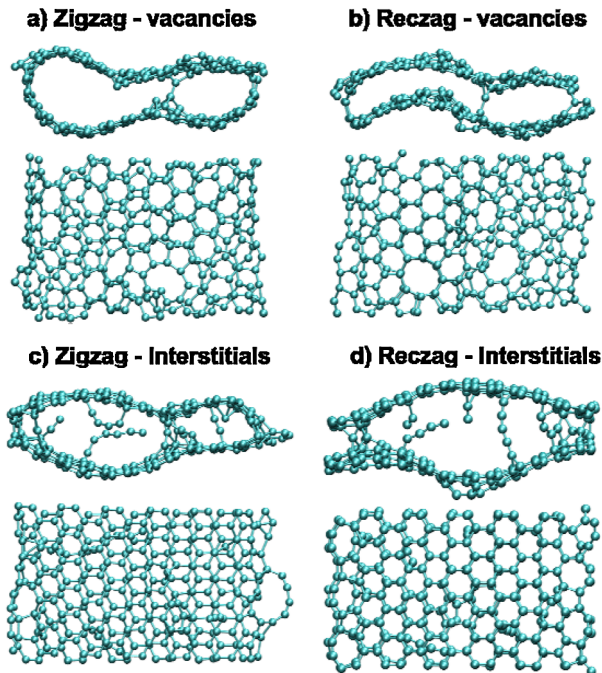


FIG. 2 (color online). Final configurations for graphene nanoribbons with vacancy (a),(b) and interstitial defects (c),(d). Zigzag ribbons create loops with both vacancies (a) and interstitials (c), while reczag edges do not show this behavior. Interstitials lead to the formation of monoatomic carbon chains in both zigzag and reczag edges, due to the low reactivity of a graphene surface.

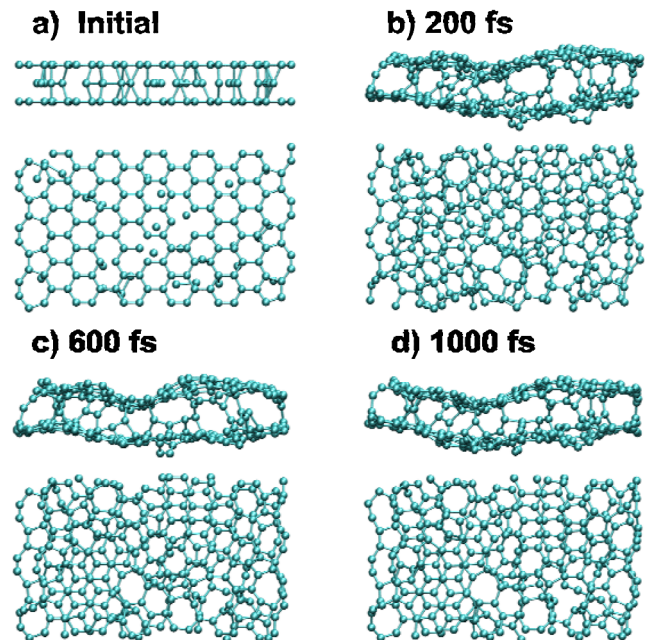


FIG. 3 (color online). Evolution of a 5-7 reczag nanoribbon with AA stacking and Frenkel pair defects (a). The high surface reactivity due to vacancies causes the interstitial atoms to readily create cross-links between the layers as early as 200 fs, as shown in (b), with very little change over the course of the simulation, as can be seen from images (c) and (d).

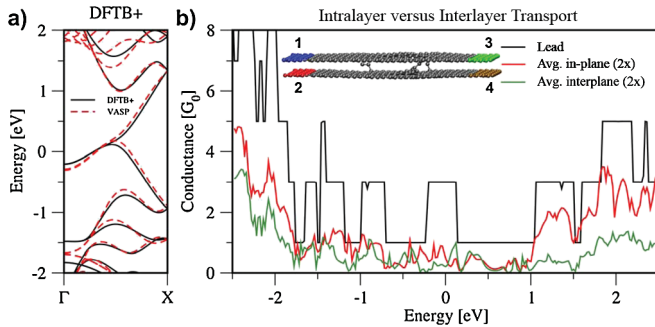


FIG. 4 (color). (a) Energy bands for the noninteracting 5-7 reczag nanoribbon leads, calculated using DFTB+ and VASP. (b) Conductance of a cross-linked reczag graphene nanoribbon bilayer. Notice the strong backscattering effect of the defects, as the in-plane conductance is strongly diminished. However, the intraplane conductance is comparable to the in-plane values around the Fermi energy.

ductance of a cross-linked graphene bilayer with 5-7 reczag edges, in which 3 links appear between the layers. We used a 4-terminal transport approach where the leads are made up of *noninteracting* semi-infinite reczag nanoribbons (Fig. 4 inset). Because of computational limitations, we used a self-consistent density functional tight binding approach. Figure 4(a) shows that the band structures computed by DFTB and DFT methods for the 5-7 reczag nanoribbon lead are very similar, confirming the validity of the approximation used [Fig. 4(a)]. For reczag nanoribbons, the computed conductance of $3G_0$ at the Fermi energy is due to the presence of two k -independent highest occupied molecular orbital states and a degenerate lowest unoccupied molecular orbital state. Figure 4 shows that strong backscattering occurs at the defective interface and the total conductance is considerably diminished. More importantly, the interplane conductance is of comparable magnitude to its in-plane counterpart. The fact that the conductance across layers is non-negligible supports the idea that cross-linking defects will be annealed easily during the Joule heating process.

Based on the above observations from DFT MD, we conclude that both vacancies and interstitials are key for keeping graphene layers parallel and preventing bilayer edge coalescence (looping), thereby providing a rationale for the absence of loop formation for electron-irradiated samples. The role of vacancies is to increase the surface reactivity and interlayer interactions far from the edges. Interstitials, on the other hand, provide effective feedstock for interlayer link creation that keeps bilayers parallel and prevents looping. Notably, it is the combination of vacancies and interstitials that accounts for keeping open edges and avoiding loop formation (coalescence of adjacent graphene layers). From quantum transport calculations, we confirm that cross-linking of bilayers increases the backscattering and creates significant transport between the layers. These cross-linking sites are key for Joule heating

defect cleansing and are susceptible to being healed during the process.

Part of this work was supported by the Center for Nanophase Materials Sciences (CNMS), sponsored by the Division of Scientific User Facilities, U.S. Department of Energy, and by the Division of Materials Science and Engineering, Basic Energy Sciences, U.S. Department of Energy. H. T. acknowledges support from the Ecole Polytechnique of Louvain. M. T. acknowledges support from the chair of excellence at Carlos III University of Madrid. The MIT authors acknowledge support from NIRT/NSF/CTS-05-06830 and Navy-ONR-MURI-N00014-09-1-1063.

- [1] K. S. Novoselov *et al.*, *Science* **306**, 666 (2004).
- [2] A. V. Krasheninnikov and F. Banhart, *Nature Mater.* **6**, 723 (2007).
- [3] J. Y. Huang *et al.*, *Proc. Natl. Acad. Sci. U.S.A.* **106**, 10 103 (2009).
- [4] J. H. Warner *et al.*, *Nature Nanotech.* **4**, 500 (2009).
- [5] A. J. R. da Silva, A. Fazzio, and A. Antonelli, *Nano Lett.* **5**, 1045 (2005).
- [6] R. H. Telling *et al.*, *Nature Mater.* **2**, 333 (2003).
- [7] P. Koskinen, S. Malola, and H. Hakkinen, *Phys. Rev. B* **80**, 073401 (2009).
- [8] C. O. Girit *et al.*, *Science* **323**, 1705 (2009).
- [9] J. A. Rodriguez-Manzo and F. Banhart, *Nano Lett.* **9**, 2285 (2009).
- [10] M. Terrones *et al.*, *Science* **288**, 1226 (2000).
- [11] M. Terrones *et al.*, *Phys. Rev. Lett.* **89**, 075505 (2002).
- [12] E. Hernández *et al.*, *Nano Lett.* **3**, 1037 (2003).
- [13] X. T. Jia *et al.*, *Science* **323**, 1701 (2009).
- [14] M. Engelund, J. A. Fürst, A. P. Jauho, and M. Brandbyge, *Phys. Rev. Lett.* **104**, 036807 (2010).
- [15] Z. Liu, K. Suenaga, P. J. F. Harris, and S. Iijima, *Phys. Rev. Lett.* **102**, 015501 (2009).
- [16] X. T. Jia *et al.*, *J. Vac. Sci. Technol. B* **27**, 1996 (2009).
- [17] G. Kresse and J. Furthmüller, *Comput. Mater. Sci.* **6**, 15 (1996); G. Kresse and J. Furthmüller, *Phys. Rev. B* **54**, 11 169 (1996).
- [18] P. E. Blöchl, *Phys. Rev. B* **50**, 17953 (1994); G. Kresse and D. Joubert, *Phys. Rev. B* **59**, 1758 (1999).
- [19] D. M. Ceperley and B. J. Alder, *Phys. Rev. Lett.* **45**, 566 (1980); N. Troullier and J. L. Martins, *Phys. Rev. B* **43**, 1993 (1991).
- [20] S. Nose, *J. Chem. Phys.* **81**, 511 (1984).
- [21] B. Aradi, B. Hourahine, and T. Frauenheim, *J. Phys. Chem. A* **111**, 5678 (2007); M. Elstner *et al.*, *Phys. Rev. B* **58**, 7260 (1998).
- [22] R. Luschtinetz *et al.*, *Surf. Sci.* **602**, 1347 (2008).
- [23] V. Meunier *et al.*, *Appl. Phys. Lett.* **81**, 5234 (2002).
- [24] C. P. Ewels *et al.*, *Phys. Rev. Lett.* **91**, 025505 (2003).
- [25] A. Stone and D. Wales, *Chem. Phys. Lett.* **128**, 501 (1986); P. A. Thrower, *Chem. Phys. Carbon* **5**, 261 (1969).
- [26] P. Koskinen, S. Malola, and H. Hakkinen, *Phys. Rev. Lett.* **101**, 115502 (2008).